Tunable UV source based on an LED-pumped cavity-dumped Cr:LiSAF laser

P. Pichon, Hussein Taleb, Frédéric Druon, Jean-Philippe Blanchot, Patrick Georges, François Balembois

Tunable UV source based on an LED-pumped cavity-dumped Cr:LiSAF laser

Pierre Pichon,[1,2,*] Hussein Taleb[1], Frederic Druon,[1] Jean-Philippe Blanchot,[2] Patrick Georges[1] and François Balembois[1].

[1]*Laboratoire Charles Fabry, Institut d'Optique Graduate School CNRS, Université Paris-Saclay, 91127, Palaiseau Cedex, France*
[2]*Effilux, 1 rue de Terre Neuve, 91940, les Ulis, France*
** pierre.pichon@institutoptique.fr*

Abstract: We developed a light-emitting diode (LED)-pumped Cr:LiSAF laser operating in Q-switched and cavity-dumped regimes. The laser produces 1.1 mJ pulses with a pulse duration of 8.5 ns at a repetition rate of 10 Hz on a broad spectrum centered at 840 nm with a full width at half maximum of 23 nm. After frequency tripling in two cascaded LBO crystals, we obtained 7 ns pulses with an energy of 13 µJ at 280 nm and with a spectral width of 0.5 nm, limited by the spectral acceptance of the phase matching process. By rotating both LBO crystals, UV emission is tuned from 276 nm to 284 nm taking advantage of the broad infrared spectrum of the Cr:LiSAF laser.

1. Introduction

With the impressive development of high-power LED in the visible, LED-pumped lasers have found a regain of interest since their first demonstration in the 1960's [1]. Initially concentrated on Nd-doped crystals [1], LED-pumped lasers using tunable media have been reported with polymers [2], fibers [3] nearly 40 years later. However, tunability has been really demonstrated only very recently on LED-pumped lasers with crystals doped with transition-metal ions like alexandrite ($Cr^{3+}:BeAl_2O_4$) with a tuning range between 715 nm and 800 nm [4], Cr:LiSAF ($Cr^{3+}:LiSrAlF_6$) between 810 nm and 960 nm [5], and Ti:sapphire ($Ti^{3+}:Al_2O_3$) between 755 nm and 845 nm [6]. In these cases, the high pump power density necessary to reach the threshold is achieved by LED-pumped Ce:YAG concentrators emitting in the yellow-orange [7]. Providing a pump power density 10 to 20 times higher than the power density of a single LED, LED-pumped concentrators have unlocked the potential of LED-pumped lasers. Compared to other pumping sources, LED-pumped concentrators combine the advantages of semi-conductors (compacity and stability), with the advantages of flashlamps (energy, robustness and low cost). They can provide an energy in the 100 mJ range and a peak power reaching 10 kW/cm^2 [6]. With such pumping parameters, LED-pumped lasers can now move from simple configurations (for example two mirror cavities) to more complex designs. The purpose of this paper is to demonstrate the next step towards complex LED-pumped laser systems. With a broad tuning range in the near infrared, LED-pumped transition-metal lasers offer many opportunities for new low-cost and very robust laser sources like ultrashort lasers, or LiDAR for atmospheric sensing, altimetry and vegetation monitoring. In addition, the 280-360 nm band can be reached by frequency conversion on purpose to detect improvised explosive devices, chemical or biologic compounds [8]. This band can be addressed by frequency doubling of alexandrite for the wavelengths higher than 350 nm and frequency tripling of Ti:sapphire or Cr:LiSAF for lower wavelengths, typically below 300 nm. In this paper, we chose to investigate an LED-pumped Cr:LiSAF because it presented much better performance than LED-pumped Ti:sapphire [5,6]. Thanks to its better spectroscopic parameters. Cr:LiSAF has often been implemented in oscillators under longitudinal pumping with Nd:lasers [9] or laser diodes [10-12] with a maximum pump power in the watt level in continuous wave. For energies reaching the mJ range [13,14] and the J range [15], some papers reported transverse pumping of Cr:LiSAF with flashlamps at low repetition rates, with the well-known drawbacks of theses pump sources (stability and lifetime). Pump pulsed operation with laser diodes were reported [16-19] including complex transverse pumping configuration including 4 laser diode stacks at 690 nm (675 W peak power each) for a total pump energy of 200 mJ during 74 µs at 10 Hz : this led to 47 mJ pulses of 300 ns in Q-switched operation in multimode operation [16]. Pulsed pumping of Cr:LiSAF with laser diodes has also been demonstrated at higher repetition rates (kHz) but with lower energies [17]. LED-pumped concentrators can provide the same range of pump energy than stacks in a simpler setup. We recently demonstrated a Cr:LiSAF oscillator emitting 8 mJ in free running operation transversally pumped by a Ce:YAG concentrator [5]. The paper presents the first active Q-switching and cavity dumped Q-switching of an LED concentrator pumped Cr:LiSAF oscillator and its frequency conversion in the ultraviolet.

2. Description of the setup

The experimental setup is reported on Fig. 1. A 5.5% doped Cr:LiSAF crystal is transversally pumped by a Ce:YAG concentrator, itself pumped by 2240 blue LEDs in a design presented elsewhere [5]. The Cr:LiSAF is 14 mm long with a section of 1x1 mm². The pump power remaining after propagation through the crystal thickness (1 mm) is reflected back into the Cr:LiSAF by a gold mirror. The Cr:LiSAF laser facets are cut at Brewster angle, with its c-axis in the plane of incidence. In order to take benefit of the strong absorption of the Cr:LiSAF on the c-axis, the pumping head is oriented in the vertical plane, perpendicular to the plane of the laser cavity . For mechanical reasons related to the size of the pumping head, the crystal is designed in a prism configuration that enables the laser beam to be in the same half space after refraction in the Cr:LiSAF. The Cr:LiSAF crystal is directly in contact with a water cooled heat sink (piece of aluminum linked to the LED's printed circuit board cooling system).

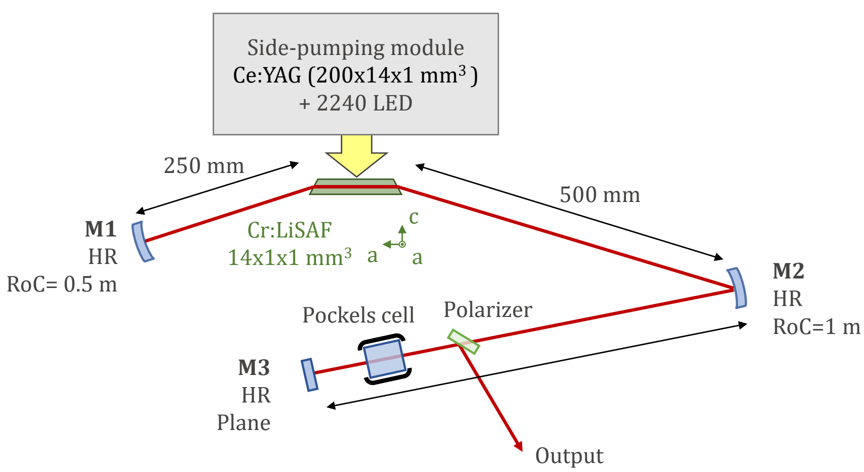

Fig. 1. Experimental setup of the LED-pumped Cr:LiSAF laser. The pumping system is perpendicular to the plane of Fig. 1 located on the top of the crystal.

For LiDAR applications, the axial resolution is related to the pulse duration. Less than 10 ns pulses are generally required to ensure an axial resolution in the meter range. This duration can hardly be obtained on simple Q-switched lasers like Cr:LiSAF which small signal gain is usually limited to values below 1.5 [5]. As a matter of fact, even in a short cavity (less than 10 cm), the pulse duration remained higher than 40 ns [5]. Hence, we choose to design a laser operating in cavity dumping as it has been previously reported with alexandrite lasers for

LiDAR applications [20]. We designed a 3-mirror cavity (Fig. 1) ensuring a TEM_{00} laser operation with the largest size possible in the Cr:LiSAF, regarding its small aperture of 1 x 1 mm². The waist is fixed to 260 µm in the first part of the cavity including the Cr:LiSAF crystal. In the second part of the cavity, the waist radius is set at 660 µm, adapted to operate with a Pockels cell in Q-switched operation. The two concave mirrors (M1 R=0.5 m and M2 R=1 m) operate at distance of half their radii of curvature from the two waists. In this configuration, the cavity length is 1.27 m corresponding to a cavity roundtrip of 8.5 ns tailored to generate sub 10 ns pulses in cavity-dumping operation.

3. Cavity-dumping in the infrared

The laser operates at a repetition rate of 10 Hz in order to reduce thermal effects occurring in the Cr:LiSAF. The pump pulse duration is adjusted to 100 µs, slightly above the fluorescence lifetime of Cr:LiSAF (67 µs). The pump duration is optimized by monitoring the fluorescence signal emitted by the Cr:LiSAF. Indeed, we observed that the amplitude of the fluorescence signal increases for pump durations up to 100 µs and then tends to decrease for longer pump pulses. This can be related to thermal quenching and to the temperature increase induced by the pump. As a matter of fact, the temperature of the Cr:LiSAF crystal is 39°C in this operating range, below thermal quenching (the temperature is controlled measuring the fluorescence lifetime). At 100 µs, the pump energy delivered by the LED-pumped concentrator is 103 mJ. Despite the poor spectral matching between Ce:YAG emission spectrum and Cr:LiSAF absorption spectrum, we estimate that an energy of 32 mJ is absorbed in the Cr:LiSAF taking into account the gold mirror reflecting the unabsorbed pump energy during the first pass in the laser crystal. Because of transverse pumping, only a part of this energy can be used by the laser beam. Considering the pump intensity profile (Fig. 2), the volume of the laser mode in the Cr:LiSAF (radius of 260µm), and the Cr:LiSAF storage lifetime, we estimate that the maximum energy that can be used at the laser wavelength is 3.4 mJ.

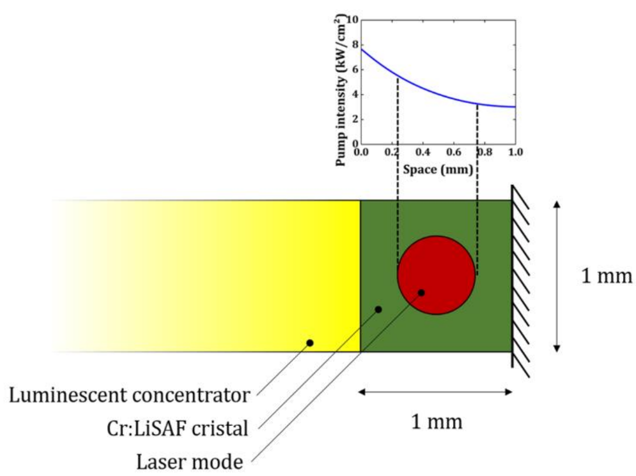

Fig. 2. Position of the laser mode in the 1 mm² section of the crystal. Inset, pump intensity distribution along the pump axis.

Before operation in cavity dumping, we tested operation in the Q-switched regime with a plane output coupler M3 having a transmission of 10 % at 850 nm. For this purpose, we inserted a KDP Pockels cell (QX-1020, Gooch & Housego) and a polarizer with a transmission of 98% for the horizontal polarization and a reflection of 80% for the vertical one. The Pockels cell is initially adjusted to be a quarter wave plate (λ/2 in double pass). The laser operation starts by applying a first step voltage transforming the Pockels cell into a half-wave plate (λ in double pass). We obtained a pulse energy of 2 mJ, a pulse duration of 135 ns and a buildup time of 530 ns. The long pulse duration in this configuration is related to the long cavity and the relatively low gain. Next, the output coupler is replaced by a highly reflective mirror. In this configuration, the buildup time is reduced to 480 ns. Once the pulse reaches its maximum, a second step voltage is applied on the Pockels cell, forcing the pulse to be ejected from the cavity by the polarizer. Fig. 3 presents the results obtained under cavity dumping. After the polarizer, we obtained pulses with an energy of 1.1 mJ. A photodiode put close to the mirror M1 gives the pulse evolution in the cavity (Fig. 3(a)). The output pulse is monitored by a second fast photodiode (rise time 1 ns). Fig. 3(b) shows few ripples after the ejection of the main pulse: this can be attributed to the residual transmission of 20% for the polarizer in the vertical polarization in the cavity axis. This means that a part of the pulse remains in the cavity after the cavity dumping, leading then to a few-10s ns small tail in the pulse as shown in fig. 3(b).

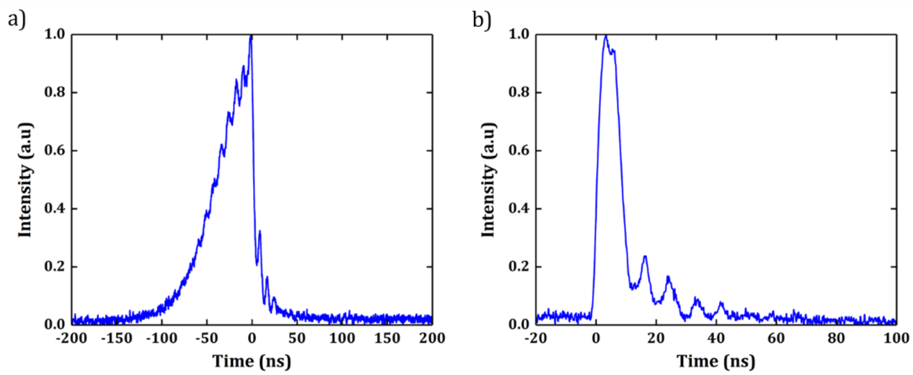

Fig. 3. a) evolution of the pulse amplification in the cavity. b) output pulse after reflection on the polarizer.

The output spectrum of the pulses after cavity dumping is plotted on Fig. 4 (measured with an Ocean Optics HR 4000 spectrometer directly on a reflection of the pulse). It is worth to note that the spectrum is 23-nm broad at FWHM (826 nm-849 nm) despite the prism shape of the Cr:LiSAF that could have induced a spectral selectivity. Indeed, due to the small dispersion index in Cr:LiSAF, the angle variation between a beam at 849 nm and a beam at 826 nm is only of 0.5 mrad after passing through the Cr:LiSAF prism. This value represents one quarter of the total divergence of the beam in this part of the cavity (full divergence of 2 mrad for a beam waist radius of 260 µm). This low deviation value explains why the Cr:LiSAF prism induces no significant spectral selectivity. Insert of Fig. 4 gives the output beam profile, very close to a TEM_{00} profile. We measured a M^2 of 1.10 in the horizontal plane and 1.13 in the vertical plane. The pulse-to-pulse stability is measured better than 10%. It is worth to note that no particular attention has been paid on the laser design to improve this stability: the laser is composed of separated mechanical mounts on a classical breadboard without air regulation.

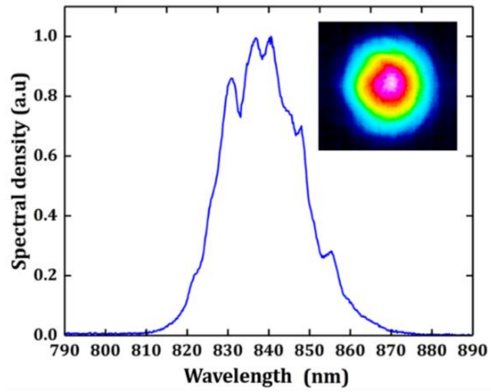

Fig. 4. Spectrum of the pulses emitted by the cavity-dumped Cr:LiSAF laser. Insert: output beam profile.

4. Frequency conversion down to the UV

The frequency conversion in the UV is obtained by frequency tripling in a two-stage cascade configuration (Fig. 5). The first stage consists in second harmonic generation (SHG) in an 8-mm-long LBO crystal. The LBO is cut in type I for SHG at 850 nm (θ = 90°, φ = 27°). The output beam for the Cr:LiSAF laser is focused by a f=100 mm lens to obtain a waist radius of 43 µm in the LBO.

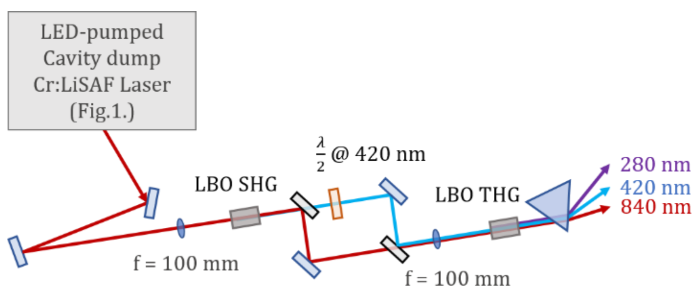

Fig. 5. Experimental setup of the frequency conversion (axial dimensions are not at scale, for the sake of legibility).

We obtained a beam with an energy of 108 µJ at 420 nm. The blue beam is measured to be circular (Fig. 6 insert), in agreement with the angular acceptance of 4.3 mrad for this phase-matching configuration, close to the divergence of the fundamental beam in the LBO crystal. The blue spectrum is measured and a bandwidth of 1.1 nm FWHM is found, which is far below the spectral width of the infrared pulses. Indeed, the blue spectrum is limited by the spectral acceptance. This also explains why the frequency conversion is only of 10% despite an IR peak power density reaching 2.2 GW/cm² in the LBO crystal. Far from being a drawback, this limited spectral acceptance can be advantageously used to tune the blue pulses. By rotating the LBO around the φ-axis, we are able to tune the blue pulses from 408 nm to 435 nm (a tunability of 9 nm FWHM plotted on Fig. 6).

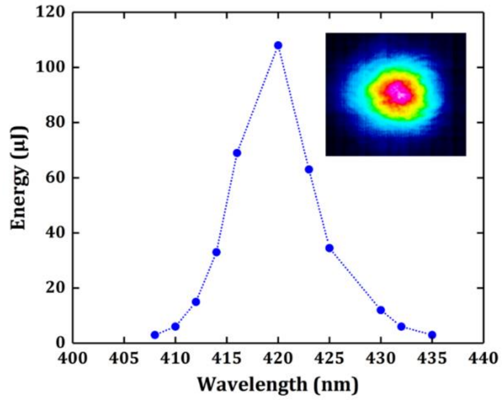

Fig. 6. Tunability of the blue pulses after SHG: energy of the pulses versus the wavelength. Insert: beam profile of the blue pulses.

The second stage of frequency conversion is realized in a 10-mm-long LBO crystal cut for sum frequency between 850 nm and 425 nm. The crystal is in type I with the following angles: θ= 90°, φ = 54.6°. This configuration imposes to rotate the blue polarization by 90° to be parallel to the infrared polarization. For this purpose, the blue and the infrared beams are separated by a dichroic mirror (HT 400-450 nm HR 800-900 nm) and then combined back by another dichroic mirror (HR 400-450 nm and HT 800-900 nm). A half waveplate is inserted in the blue beam path to rotate its polarization. The beam waist in the first LBO crystal is re-imaged in the second one using a 2f-2f configuration with a f=100 mm lens. After wavelength separation by a UV silica prism, we are able to characterized the UV beam. In the optimal configuration, we found an energy of 13 µJ at 280 nm, corresponding to the third harmonic generation (THG) of the peak of the infrared spectrum at 840 nm. This is a 1.2% efficiency limited by the spectral acceptance. The UV average power is measured with a Gentec thermal powermeter (noise in the 10 µW range), the measurement is performed with and without phase matching to be sure that the background noise and other wavelengths are subtracted. The pulse to pulse stability in the UV is measured to be 21%. We measured a spectral bandwidth of 0.5 nm (Fig. 8). The pulse duration is measured with a fast photodiode. We found a value of 7 ns FWHM (Fig. 7(b)). By tailoring the rotation of the two LBO crystals, it is possible to tune the UV from 276 nm to 284 nm.

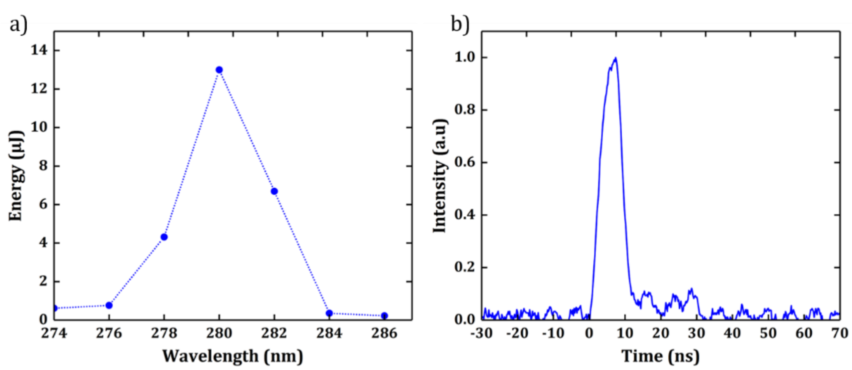

Fig. 7. a) Tunability of the UV pulses after THG: energy of the pulses versus the wavelength. b) output pulse in the UV.

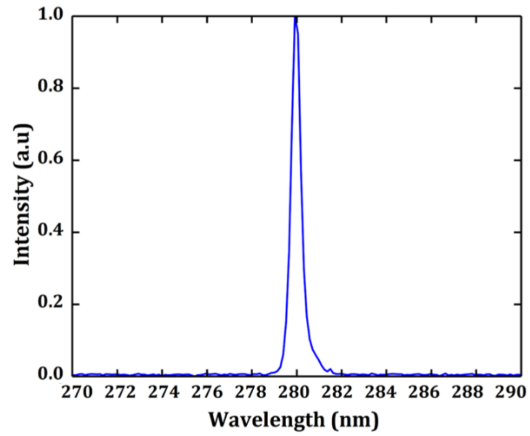

Fig. 8. Spectrum of the UV pulse after THG.

5. Conclusion

To conclude, an LED-pumped Cr:LiSAF laser operating in cavity-dumping is reported for the first time. We obtain 1.1 mJ pulses at 10 Hz with a pulse duration of 8.5 ns. After a first SHG stage in an LBO crystal, pulses with an energy up to 108 µJ at 420 nm are demonstrated with a Gaussian beam profile. After a second THG stage in a second LBO, the laser produced 7 ns pulses with an energy up to 13 µJ at 280 nm, a gaussian beam profile and a tunability over 8 nm. This new source can be seen as an alternative to classical sources covering this wavelength range in the UV with the appropriate parameters (kW peak power, ns pulse duration, good beam quality and tunability) relying on relatively complex and onerous pump systems. For instance OPO pumped by frequency quadrupled Nd:YAG lasers can cover the 300-2340 nm range [21]. Similarly, Ce:LiCAF laser oscillators pumped by Nd:YAG 4th harmonic can reach the 280-300 nm range [22]. In order to increase the efficiency of the frequency conversions, the wavelength of the fundamental pulse can be narrowed with a birefringent filter or an etalon. Also, broader tuning range in the UV can be obtained tuning the fundamental pulse. In this work, the simplicity of the source is required for the application. Tuning the fundamental would break the simplicity of this source as this requires alignment of the cavity and of the non-linear conversion processes. Frequency tripling of Cr:LiSAF has already been proposed as a solution for this wavelength range [23-25]. In [24], with a pump energy of 60 J from flashlamps at 1 Hz, laser pulses of 20 ns at 840 and an energy of 120 mJ are generated, this led to 20 mJ pulses in the blue and 6 mJ in the UV. This is the first time that a LED pumped laser source can be considered for a real application as the performance achieved in the UV are convenient for middle range LiDAR applications. Namely, the detection range being proportional to the squareroot of the pulse energy, 10 µJ UV pulses can be useful to detect improvised explosive devices up to a range of 100 m with meter axial resolution. In addition, this cavity dumped oscillator can be easily transformed in a regenerative amplifier seeded by femtosecond pulses. The spectral width obtained in free running (23 nm FWHM) proves that this amplifier could support less than 50 fs pulses at 850 nm with a potential to reach the mJ range. Moreover, energy scaling can be easily achieved by increasing the concentrator dimensions and the Cr:LiSAF length. As Ce:YAG crystals are large size and low cost crystals and as 10 cm long Cr:LiSAF are common for flashlamp systems, LED pumped Cr:LiSAF systems has the potential to deliver 10-100 mJ pulses. Consequently, this work opens the route to a new generation of high energy femtosecond amplifiers with unique properties of simplicity, robustness, long lifetime and stability.

Funding : Agence Nationale de la Recherche and Direction Générale de l'Armement (ANR-17-ASTR-0021).

References

1. R. B. Allen and S. J. Scalise, "Continuous operation of a YAG:Nd laser by injection luminescent pumping," Appl. Phys. Lett. **14**, 188-190 (1969).
2. Y. Yang, G. a. Turnbull, and I. D. W. Samuel, "Hybrid optoelectronics: A polymer laser pumped by a nitride light-emitting diode," Appl. Phys. Lett. **92**, 163306 (2008).
3. L. Htein, W. Fan, P. R. Watekar, and W.-T. Han, "Amplification by white light-emitting diode pumping of large-core Er-doped fiber with 12 dB gain," Opt. Lett. **37**, 4853-4855 (2012).
4. P. Pichon, A. Barbet, F. Druon, J.-P. Blanchot, F. Balembois, and P. Georges, "LED-pumped alexandrite laser oscillator and amplifier," Opt. Lett. **42**, 4191-4194 (2017).
5. P. Pichon, A.Barbet, J.-P. Blanchot, F.Druon, F. Balembois, and P. Georges, "LED-pumped passively Q-switched Cr:LiSAF laser," Opt. Lett. **43**, 4489-4492 (2018).
6. P. Pichon, A.Barbet, J.-P. Blanchot, F.Druon, F. Balembois, and P. Georges, "Light-emitting diodes: a new paradigm for Ti:sapphire pumping," Optica **5**, 1236-1239 (2018).
7. A. Barbet, A. Paul, T. Gallinelli, F. Balembois, J.-P. Blanchot, S. Forget, S. Chénais, F. Druon, and P. Georges, "Light-emitting diode pumped luminescent concentrators: a new opportunity for low-cost solid-state lasers," Optica **3**, 465-468 (2016).
8. K. L. Gares, K. T. Hufziger, S.V. Bykov, and S.A. Asher, "Review of explosive detection methodologies and the emergence of standoff deep UV resonance Raman," J. Raman Spectrosc **47**, 124-141 (2016).
9. L. Kunpeng, S. Yanlong, Y. Li, C. Hongwei, C. Shaowu, T. Mengmeng, and Y. Aiping, "High-efficiency tunable dual-wavelength Cr:LiSAF laser with external grating feedback," Opt. Commun **405**, 233-237 (2017).
10. U. Demirbas, J. Wang, G. S. Petrich, S. Nabanja, J. R. Birge, L. A. Kolodziejski, F. X. Kärtner, and J. G. Fujimoto, " 100-nm tunable femtosecond Cr:LiSAF laser mode locked with a broadband saturable Bragg reflector," App. Opt. **56**, 3812-3816 (2017).
11. A. Dergachev, J. H. Flint, Y. Isyanova, B. Pati, E. V. Slobodtchikov, K. F. Wall, and P. F. Moulton, "Review of multipass slab laser systems," IEE J. Sel. Top. Quantum Electron, **13**, 647-660, (2007).
12. U. Demirbas and I. Baali, "Power and efficiency scaling of diode pumped Cr:LiSAF lasers: 770-1110 nm tuning range and frequency doubling to 387-463 nm," Opt. Lett. **40**, 4615-4618 (2015).
13. Martin Stalder, Bruce H. T. Chai, and Michael Bass, "Flashlamp pumped Cr:LiSrAlF6 laser,", Appl. Phys. Lett. **58**, 216-218 (1991).
14. R. E. Samad, S. L. Baldochi, G. E. C. Nogueira, and N. D. Vieira, Jr, "30 W Cr:LiSrAlF6 flashlamp-pumped pulsed laser," Opt. Lett. **32**, 50-52 (2007).
15. D. E. Klimek and A. Mandl, "Power scaling of a flashlamp-pumped Cr:LiSAF thin-slab zig-zag laser," IEEE J. Quantum Electron, **38**, 1607-1613 (2002).
16. G. H. Kim, R. D. Mead, J. W. Pierce, M. S. Bowers, L. B. Kulesa, J. A. Skidmore, B. L. Freitas, and N. P. Barnes, "High energy diode-pumped, Q-switched Cr:LiSAF laser," ASSL proceeding, (1998).
17. U. Demirbas and D.A.E. Acar, "Continuous-wave, quasi-continuous-wave, gain-switched, and femtosecond burst-mode operation of multi-mode diode-pumped Cr:LiSAF lasers", J. Opt. Soc. Am. B **33**, 2105-2113 (2016).
18. C. C. Johnson, D. J. Reichle, and N. P. Barnes, "High energy diode side-pumped Cr:LiSAF laser," Proceedings of ASSL (1996).
19. V. A. Fromzel, V. V. Ter-Mikirtychev, J. S. Smucz, and C. R. Prasad, "Diode-pumped, tunable, narrow linewidth Cr:LiSAF lasers for water vapor differential absorption lidars," Proceedings of SPIE, 4378 (2001).
20. G. M. Thomas, A. Minassian, X. Sheng, and M. J. Damzen, "Diode-pumped Alexandrite lasers in Q-switched and cavity-dumped Q-switched operation," Opt. Express **24**, 27212-27224 (2016).
21. N.V Konndrtyuk, A.A Shagov, K.L Demidchik, A.M Yurkin, and A.E Kokh, "BBO-crystal optical parametric oscillator tunable over the 300-2340 nm range and pumped by the 4th harmonic of a Nd:YAG laser," Quantum Electron. **30**, 253-254 (2000).
22. M. H Pham, M. Cadatal-Raduban, D. V. Pham, T. X. Nguyen, M. V. Luong, K. Yamanoi, T. Shimizu, N. Sarukura, and H. D. Nguyen, "Tunable narrow linewidth picosecond pulses from a single grating gain-switched Ce:LiCAF laser," Laser Phys. **28**, 085802 (2018).
23. F. Balembois, M. Gaignet, F. Louradour, V. Couderc, P. Georges, and A. Brun, "Tunable picosecond UV source at 10 kHz based on an all solid-state diode-pumped laser system," Appl. Phys. B, **65**, 255-258 (1997).
24. J. F. Pinto, L. Esterowitz, and G. H. Rosenblatt, "Frequency tripling of a Q-switched Cr:LiSAF laser to the UV region," IEEE J. Sel. Top. Quantum Electron **1**, 58-61 (1995).
25. J. F. Pinto and L. Esterowitz, "Unstable Cr:LiSAF laser resonator with a variable reflectivity output coupler," Appl. Opt. **37**, 3272-3275 (1998).